Insight in chitosan aerogels derivatives - Application in catalysis

Ronan Le Goff, Olivier Mahé, Ronan Le Coz-Botrel, Sylvie Malo, Jean-Michel Goupil, Jean-François Brière, Isabelle Dez

Insight in chitosan aerogels derivatives - Application in catalysis

Ronan Le Goff[a], Olivier Mahé[b], Ronan Le Coz-Botrel[a], Sylvie Malo[c], Jean-Michel Goupil[d], Jean-François Brière[b] and Isabelle Dez[a]

[a]Normandie Univ, ENSICAEN, UNICAEN, CNRS, LCMT, 14000 Caen, France.

[b]Normandie Univ, UNIROUEN, INSA Rouen, CNRS, COBRA, 76000 Rouen, France.

[c]Normandie Univ, ENSICAEN, UNICAEN, CNRS, CRISMAT, 14000 Caen, France.

[d]Normandie Univ, ENSICAEN, UNICAEN, CNRS, LCS, 14000 Caen, France.

Abstract Thanks to an aerogel formulation, an efficient heterogeneous modification of chitosan is described and offers the convenient covalent-functionalisation of primary amine of insoluble microspheres into secondary benzylic-amines with various functionalities. The SEC, XRD and textural analyses provided a better insight into the chitosan aerogels and showed that this synthetic process allows high substitution ratio (> 80%) without depressing the desirable properties of the well-defined chitosan macromolecular structure. As a proof of principle, original catalytic chitosan aerogels flanked by a phosphine-pendant were prepared and applied successfully in the heterogenous pallado-catalysed allylic substitution reaction.

Keywords : Chitosan aerogel, Reductive amination, Textural properties, Heterogeneous catalysis

1- Introduction

Chitosan is a linear polysaccharide which consists of *D*-glucosamine and *N*-acetyl-*D*-glucosamine motifs. This material is obtained by deacetylation of chitin, the second more abundant and widely distributed natural polymer on earth [1-3]. Chitosan have many prominent biological properties like biodegradability [4, 5], biocompatibility [6-8], non-toxicity [9-12] and antibacterial activity [11-15]. This polysaccharide proved to be useful as a natural electrolyte due to the protonation of the amino functional groups in acidic conditions [16]. Thanks to the β-(1→4) linked D-glucosamine repeating units with three reactive groups, the highly regular structure of chitosan offers various opportunities for designing advanced

materials by means of chemical modifications. In particular, the regioselective and quantitative modification is the most promising way to provide novel chitosan derivatives with useful properties [17, 18], in spite of revealing synthetic challenging. The chemical modification of transiently solubilized-chitosan macromolecules, either by protonation of the NH_2 or protection of some functions, is the common way to reach this goal. However, these strategies often required harsh reaction conditions, which lead to partial degradation of the macromolecular structure [19-21] and impact its intrinsic properties, including solubility, viscosity, and appearance [20, 22]. On the other hand, the more promising heterogeneous functionalisation strategy is still limited ought to the difficult accessibility of the functional groups within the macromolecule, which eventually affords modification distributions with a lack uniformity [23-25]. Therefore, the development of a new strategy allowing a heterogeneous modification of chitosan without affecting its desirable properties would be of high-value. Over the past decade, particular attention was paid to chitosan aerogel and its composites for their unique applications in catalysis, biomedical uses and removal of pollutants [26]. These materials are obtained from supercritical CO_2 drying process of chitosan alcogels giving rise to porous architectures with large surface areas (over 100 $m^2.g^{-1}$). Consequently, a significant amount of chitosan amino functional groups becomes accessible for chemical modifications as a result of the open-pore structure of the polymeric network [27]. Furthermore, the high surface area of chitosan aerogel and the accessibility of functionality derived thereof enhance the properties of the materials for drug delivery [28], adsorption of heavy metal ions [29, 30], and for the catalytic applications [31-34]. Finally, the well-defined structure of chitosan aerogel in term of molecular weight distribution, surface area and accessibility of the amine functions guarantees a better reproducibility for the target applications compared with commercial chitosan powder.

Taking advantages of the properties of chitosan aerogels [35], Quignard and collaborators have shown the possibility to form imine functionalities from the corresponding aldehydes with a high degree of substitution. We became interesting in the versatile subsequent reduction of imine functional group to eventually obtained mono-substituted amine derivatives. Despite this sequence was previously tackled in an acidified methanolic suspension power chisosan [36], this process led to moderate substitution ratio. We are pleased to report herein a heterogeneous modification of the amine moieties by means of a reductive amination process providing high substitution rate, while keeping the intrinsic properties of the of chitosan aerogels, as testify by the evaluation of textural properties, by SEC and XRD analyses. A variety of benzylic-

functional groups were covalently introduced and an original application the palladium-catalyzed allylic substitution was allowed thanks to a phosphine-substituted material.

2- Materials and methods

2.1 Materials

Et_2O, DCM, THF and MeCN were purified by a Pure Solv-MD 5 Solvent Purification System (activated alumina column containing a copper catalyst and molecular sieves). Anhydrous THF and MeCN were degassed (freeze-pump) before use. Absolute EtOH was used without further purification for Schiff Base formation and for chitosan and chitosan derivatives aerogel beads formation. MeOH was dried over 3Å molecular sieves when implied as solvent in the reduction step [37]. 1,2-DCE was purchased in 99% grade from Alfa-Aesar and dried over 3Å molecular sieves before use. Chitosan middle-viscous (Mv = 336,000 $g.mol^{-1}$; DA = 20%) was purchased from Sigma-Aldrich. Commercially available reagents p-tolualdehyde (Janssen; 97%), methyl 4-formylbenzoate (Alfa-Aesar; 99%), p-anisaldehyde (Fisher-Acros; 99%), 4-(4,4,5,5-tetramethyl-1,3,2-dioxaborolan-2-yl)-benzaldehyde (Fisher-Acros; 97%), 1,3-dibromobenzene (Fisher-Acros; 97%), butyl lithium (Sigma-Aldrich; 1.6M solution in hexane), sodium triacetoxyborohydride (Fisher-Acros; 97%), sodium cyanoborohydride (Fisher-Acros; 95%), tetrabutylammonium borohydride (Sigma-Aldrich; 98%), 4-(dimethylamino)pyridine (DMAP) (Sigma-Aldrich; ≥99%), bromobenzene (Sigma-Aldrich; 99%), magnesium (Sigma-Aldrich; 99%), iodine (Fisher-Acros; 99%), acetic anhydride (Sigma-Aldrich; 99%), *N*,*O*-bis(trimethylsilyl)acetamide (Fisher-Acros; 95%), potassium acetate (Sigma-Aldrich; ≥99%), Allylpalladium(II) chloride dimer (Sigma-Aldrich; 98%) were used without further purification. Chlorodiphenylphosphine, dimethylformamide, cinnamaldehyde, trimethylamine, dimethyl malonate **5** were distilled before use.

Thin layer chromatography (TLC) was performed on silica gel 60-F254 plates (0.1 mm) from Merck with UV detection. Chromatographic purifications were conducting using Merck silica gel Si 60 (40-63 μm). CO_2 supercritical drying process was carried out with a Critical Point Dryer Polaron E3100. NMR spectra were recorded on a Bruker Avance III 400 at room temperature in $CDCl_3$ for organic compounds and on a Bruker Avance III 500 at 70°C in a D_2O/DCl mixture for chitosan derivatives. ^1H and ^{13}C NMR chemical shifts (δ) are reported in ppm using the residual peak of chloroform-*d* (7.26 for ^1H NMR; 77.16 ppm for ^{13}C NMR) or water (4.79 for ^1H NMR). Coupling constants (*J*) are reported in Hertz (Hz). The following abbreviations were used to explain the multiplicities: s = singlet, d = doublet, t = triplet, q =

quartet, m = multiplet, bs = broad singlet. Solid-state MAS NMR (Magic Angle Spinning Nuclear Magnetic Resonance) spectroscopy has been performed on a Bruker Avance III spectrometer using a 4 mm double resonance probe. The spectra has been obtained using 90° single-pulse with a duration of 2.26 μs, a recycling delay of 5 s and a spinning rate of 9 kHz. InfraRed spectra were recorded on a Perkin Elmer Spectrum One FT-IR spectrometer equipped with an ATR device, and only the strongest or structurally most important peaks are listed in cm^{-1}. High Resolution Mass Spectrometry was performed on a Q-TOF Xevo G2-XS WATERS spectrometer. Surfaces areas were determined by N_2 physisorption at 77K using an ASAP 2020 Micromeritics apparatus. The powdered sample (200 mg) was evacuated overnight at 353K prior N_2 adsorption. The total porous volume V_{pore} is dertermined from the volume adsorbed under relative pressure of 0.99. High resolution X-ray powder diffraction data were collected using a D8 Advance Vario 1 Brucker diffractometer (θ-2θ Bragg-Brentano mode) equipped with a Cu X-ray tube (λ = 1.540598 Å), a Ge (111) monochromator (Johansson type) and a Lynx Eye detector. XRD data were collected over a [4°-40°] 2θ range with an angular increment of 0.0105°, and a step time of 2 seconds (20 h/scan) at room temperature. The crystallinity index (CrI) of the chitosan samples was determined according to the method of Focher et al. [38] using the equation: $CrI_{110} = (I_{110} - I_{am}) / I_{110} \times 100$; where I_{110} is the maximum intensity (2θ = 20°) of the (110) lattice diffraction and I_{am} is the intensity of amorphous diffraction at 2θ = 16° of chitosan.

The absolute determination of weight and number average molar masses (respectively, Mw and Mn) of chitosan and Schiff base chitosan aerogels **1** and **2a** were performed by coupling on-line a size exclusion chromatography (SEC), a multi-angle laser light scattering (MALLS) and a differential refractive index detector (DRI). Acetic acid/acetate buffer (pH 4.7) and $LiNO_3$ 0.1 M used as carrier, was eluted at 0.5 $mL.min^{-1}$ flow rate (Flom HPLC pump 301). The SEC-MALLS technic has been described elsewhere [39]. The concentration of each eluted fraction have been determined with the DRI (Shimadzu RID-6A, Japan) according to the known value of dn/dC (0.19 $mL.g^{-1}$).

2.2 Preparation of chitosan aerogel beads

1g of chitosan was suspended in 100 mL of a solution of acetic acid (0.055 M, 330 μL of AcOH in nearly 99.67 mL of ultrapure water) and stirred for 16 h at room temperature. The chitosan solution was then filtered on a glass filtering funnel and filtrate was standing for 30 minutes until no more bubbles remains. The filtrate was then dropped into a 1 liter sodium hydroxide

solution (10 g of NaOH in 1 L of ultrapure water) through a 0.8 mm gauge syringe needle and the suspension was slowly stirred for another 3 hours. Chitosan beads were then dehydrated by successive immersion in a series of water-ethanol baths of increasing alcohol concentration (10, 30, 50, 70, 90 and 100%; 15 min in each bath). Chitosan beads were finally dried under supercritical CO_2 conditions to give the corresponding aerogel material.

2.3 Typical procedure for the functionalisation of chitosan aerogel beads.

Chitosan aerogel beads **1** (25 mg, 0.127 mmol, 1 eq) were suspended in 1.2 mL of an ethanol solution of aldehyde (0.508 mmol for 4 eq or 0.254 mmol for 2 eq of aldehydes **a**-**e**) and heated at 60°C without stirring. After 24h, the suspension was cooled to room temperature and the solvent was removed. Chitosan Schiff base beads, recovered quantitatively, were washed 5 times by successive immersion in 1.2 mL of an ethanol baths (15 min of orbital shaking at 750 rpm for each bath). The beads were finally dried under supercritical CO_2 conditions.

The beads of Chitosan Schiff base **2a**-**2e** (5 mg, 1 eq) were placed into a 1.2 mL vial. The vial was purged with argon for 10 min before the addition of 400 µL of anhydrous methanol. A very low amount of phenol red indicator (it gives a yellow coloration for pH below 6.8 and a red one above 8.2) was added and the suspension was slowly stirred for 2 min. DMAP was added to the yellow suspension until its coloration turned to red. Finally the pH was adjusted (turned to yellow coloration) with a small amount of acetic acid. $NaBH_3CN$ (6 eq) was added to the suspension and the vial was slowly stirred at room temperature. Addition of another amount of acetic acid could be necessary to adjust pH during the reaction (coloration turning to orange/red). After 48h, solvent was removed and beads were washed 5 times by successive immersion in 1.2 mL ethanol bath (15 min of orbital shaking at 750 rpm for each bath). The chitosan amine derivatives beads **3a**-**3e**, recovered quantitatively, were finally dried under supercritical CO_2 conditions.

2.4 General Procedure for Pd-Catalysed Allylic Substitution of (E)-1,3-Diphenyl-3-acetoxyprop-1-ene with Dimethyl Malonate or morpholine [40]

Chitosan phosphine Schiff base beads **2e** (8.7 mg, 0.0215 mmol, 0.043 eq) and $[PdCl(C_3H_5)]_2$ (2.7 mg, 0.0075 mmol, 0.015 eq) were placed into a Schlenk. The Schlenk was purged three times (vacuum then argon) then 500 µL of anhydrous and degassed MeCN were added. The suspension was stirred slowly at room temperature for 1h. KOAc (0.5 mg, 0.005 mmol, 0.01 eq), BSA (370 µL, 1.5 mmol, 3 eq), a solution of (E)-1,3-diphenylallyl acetate **4** (126 mg, 0.5

mmol, 1 eq) in 700 µL of anhydrous and degassed MeCN and dimethyl malonate **5** (1.5 mmol, 3 eq) as nucleophile were successively added. Then the suspension was slowly stirred at room temperature for 24h. Solvent was removed and beads were washed three times with 900µL of anhydrous and degassed MeCN (15 min of stirring for each). Solutions were gathered and concentrated under vacuum. The crude mixture was purified by flash chromatography (SiO_2; 9:1 pentane/AcOEt) to yield **6** as colorless oil (118 mg, 73%).

2.5 Charaterisation of chitosan aerogel beads functionalisation.

The determination of substitution degree (DS) for both Schiff Base formation and reduction steps have been performed by NMR analysis in a mixture D_2O/DCl (78 µL of 20 w% solution of DCl + 920 µL of D_2O) at 70°C. In the case of Schiff bases, DS_{imine} were calculated using integrals of aromatic protons from free aldehydes (obtained by hydrolysis of imine moieties during NMR samples preparation) and anomeric proton from glucosamine units. In the case of secondary amines, DS_{amine} were calculated using integrals of both anomeric protons of glucosamine and N-benzyl glucosamine units.

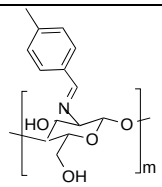 **2a**	**Chitosan Schiff base 2a** DS_{imine} = 92-99%. IR (neat): ν = 1636 (C=N), 1065, 1023, 812 (C-H_{Ar}) cm^{-1}.
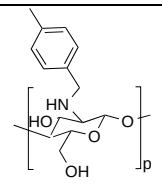 **3a**	**Chitosan secondary amine 3a** DS_{amine} = 81-82%. IR (neat): ν = 1065, 1022, 806 (C-H_{Ar}) cm^{-1}. ^{1}H NMR (500MHz, D_2O): δ = 7.80 (d, J = 7.6 Hz, H_{Ar}), 7.74 (d, J = 7.6 Hz, H_{Ar}), 5.69-5.34 (m, $H_{anomeric\ secondary\ amine}$), 5.30-5.22 (m, $H_{anomeric\ glucosamine}$), 4.91-4.75 (m), 4.56-4.47 (m), 4.38-4.26 (m), 4.23-4.13 (m), 3.74-3.57 (m), 2.76 (s, Me), 2.46 (s, Me_{Ac}).
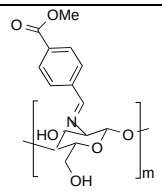 **2b**	**Chitosan Schiff base 2b** DS_{imine} = 98-99%. IR (neat): ν = 1715 (C=O), 1643 (C=N), 1282 (C-O), 1109, 1069, 1045, 1016, 766 (C-H_{Ar}) cm^{-1}.
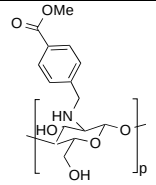 **3b**	**Chitosan secondary amine 3b** DS_{amine} = 67-74%. IR (neat): ν = 1713 (C=O), 1282 (C-O), 1108, 1067, 1019, 763 (C-H_{Ar}) cm^{-1}. ^{1}H NMR (500MHz, D_2O): δ = 8.41 (bs, H_{Ar}), 7.97 (d, *J* = 7.3 Hz, H_{Ar}), 5.51-5.36 (m, $H_{anomeric\ secondary\ amine}$), 5.30-5.22 (m, $H_{anomeric\ glucosamine}$), 5.07-4.56 (m), 4.34-4.22 (m), 4.21-4.07 (m), 3.68 (s, OMe), 3.67-3.50 (m), 2.40 (s, Me_{Ac}).

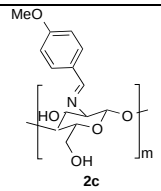 **2c**	**Chitosan Schiff base 2c** DS_{imine} ≥99%. IR (neat): ν = 1605 (C=N), 1514, 1253 (C-O), 1168, 1065, 1024, 830 (C-H_{Ar}) cm^{-1}.
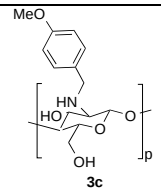 **3c**	**Chitosan secondary amine 3c** DS_{amine} = 83-87%. IR (neat): ν = 1514, 1247 (C-O), 1064, 1027, 816 (C-H_{Ar}) cm^{-1}. ^{1}H NMR (500MHz, D_2O): δ = 7.79 (d, *J* = 7.6 Hz, H_{Ar}), 7.41 (d, *J* = 7.6 Hz, H_{Ar}), 5.49-5.29 (m, $H_{anomeric\ secondary\ amine}$), 5.28-5.17 (m, $H_{anomeric\ glucosamine}$), 5.02-4.62 (m), 4.49-4.36 (m), 4.33-4.20 (m), 4.17 (s, OMe), 4.15-4.00 (m), 3.68-3.50 (m), 2.39 (s, Me_{Ac}).
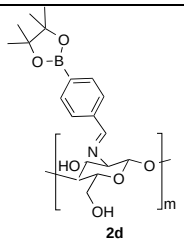 **2d**	**Chitosan Schiff base 2d** DS_{imine} ≥95%. IR (neat): ν = 1641 (C=N), 1360 (B-O), 1143 (C-O), 1082, 1067, 1019, 857 (C-H_{Ar}) cm^{-1}.
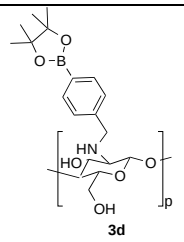 **3d**	**Chitosan secondary amine 3d** DS_{amine} = 86-89%. IR (neat): ν = 1360 (B-O), 1143 (C-O), 1082, 1068, 1020, 857 (C-H_{Ar}) cm^{-1}. ^{1}H NMR (500MHz, D_2O): δ = 8.17 (d, *J* = 6.8 Hz, H_{Ar}), 7.86 (d, *J* = 6.9 Hz, H_{Ar}), 5.53-5.30 (m, $H_{anomeric\ secondary\ amine}$), 5.30-5.16 (m, $H_{anomeric\ glucosamine}$), 5.04-4.60 (m), 4.54-3.84 (m), 3.69-3.46 (m), 2.38 (s, Me_{Ac}), 1.52 (s, $Me_{pinacol}$).
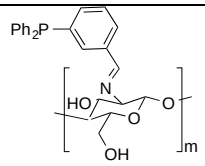 **2e**	**Chitosan Schiff base 2e** DS_{imine} = 97-98%. IR (neat): ν = 1644 (C=N), 1434 (P-C_{Ar}), 1147, 1067, 1041, 1026, 742 (C-H_{Ar}), 684 (C-H_{Ar}) cm^{-1}.
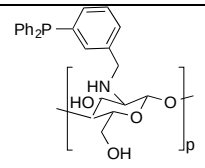 **3e**	**Chitosan secondary amine 3e** IR (neat): ν = 1434 (P-C_{Ar}), 1147, 1067, 1041, 1026, 742 (C-H_{Ar}), 684 (C-H_{Ar}) cm^{-1}.

3. Results and discussion

3.1 Functionalisation of chitosan aerogels

The heterogeneous chitosan modification was performed from the previously prepared chitosan aerogels **1** (*vide infra*) as starting material, and was carried out in a two-steps reductive amination reaction (Scheme 1).

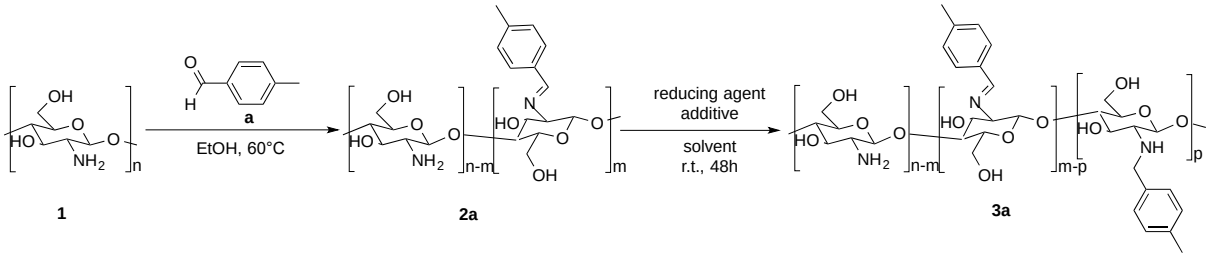

Scheme 1. Model reaction for chitosan aerogels modifications

In line with Quignard pioneering investigation on chitosan aerogels [35], the imine formation took place uneventfully in EtOH given that an excess of *p*-tolualdehyde **a** (4 equivalents) was used at 60°C in order to secure both a reasonable reaction rate and a high substitution degree (DS_{imine}) of 95% determined by NMR (Figure 1). With respect to FTIR spectra, the formation of imino chitosan **2a** was confirmed by the presence of the imino band at 1636 cm^{-1}, and the characteristic bands for the aromatic region at 1065, 1023, 812 cm^{-1}. Then, the heterogeneous reduction of imine derivatives **2a** into benzylated-product **3a** was undertaken (Table 1).

Table 1: Conditions of reduction of Schiff base **2a**

Entry	Reducing agent (eq.)	Additive (eq.)	Solvent	DS_{amine} [a]
1	$NaBH(OAc)_3$ (6)	-	MeOH	16%
2	$NaBH(OAc)_3$ (6)	AcOH (2)	1,2-DCE	51%
3	$(nBu)_4NBH_4$ (1.5)	-	1,2-DCE	36%
4		AcOH (4.5)[b]	1,2-DCE	81%
5	$NaBH_3CN$ (6)	AcOH (2)	1,2-DCE	32%
6	$NaBH_3CN$ (6)	-	MeOH	82%

[a] DS_{amine} of the obtained Bn-amine **3a** determined by ^1H NMR in DCl/D_2O at 70°C. [b] *in situ* formation of $(nBu)_4BH(OAc)_3$ by mixing $(nBu)_4BH_4$ and AcOH in 1:3 ratio.

Various acid-stable reducing agents were tested at room temperature for 48h. $NaBH(OAc)_3$ furnished a better reduction ratio to reach a DS_{amine} of 51% in the presence of acetic acid (entries 1 and 2). The more soluble $(nBu)_4BH(OAc)_3$, formed in situ by mixing $(nBu)_4BH_4$ and AcOH, allowed an excellent 81% DS_{amine} (entries 3 and 4). Interestingly, the commercially available $NaBH_3CN$ led to 82% DS_{amine} in MeOH without the need of acetic acid additive. This is an important achievement as long as an early hydrolysis of the imine moieties favored by AcOH was met in some experiments giving some reproducibility issues. This phenomenon was reduced by working in 1,2-dichloroethane (DCE) instead of MeOH for $NaBH(OAc)_3$ for instance, but proved to be ineffective for $NaBH_3CN$ (entries 4 versus 5). The representative ^1H

NMR spectra of **3a** (Figure 1) demonstrate the efficacy of the $NaBH_3CN$ protocol in MeOH. Importantly, Cabrera-Escribano and co-workers described an interesting reduction of imine-derived chitosan as suspension powder in the presence $NaBH_3CN$ and AcOH, but with a lower substitution ratio, showing the advantage of using aerogel materials ~~[39]~~ [36]. Furthermore, the resulting aerogel materials, either in the form of imine or amine (**2a-3a**) were conveniently recovered by simple filtration. However, the impact on the texture of the functionalized material was an issue to be questioned.

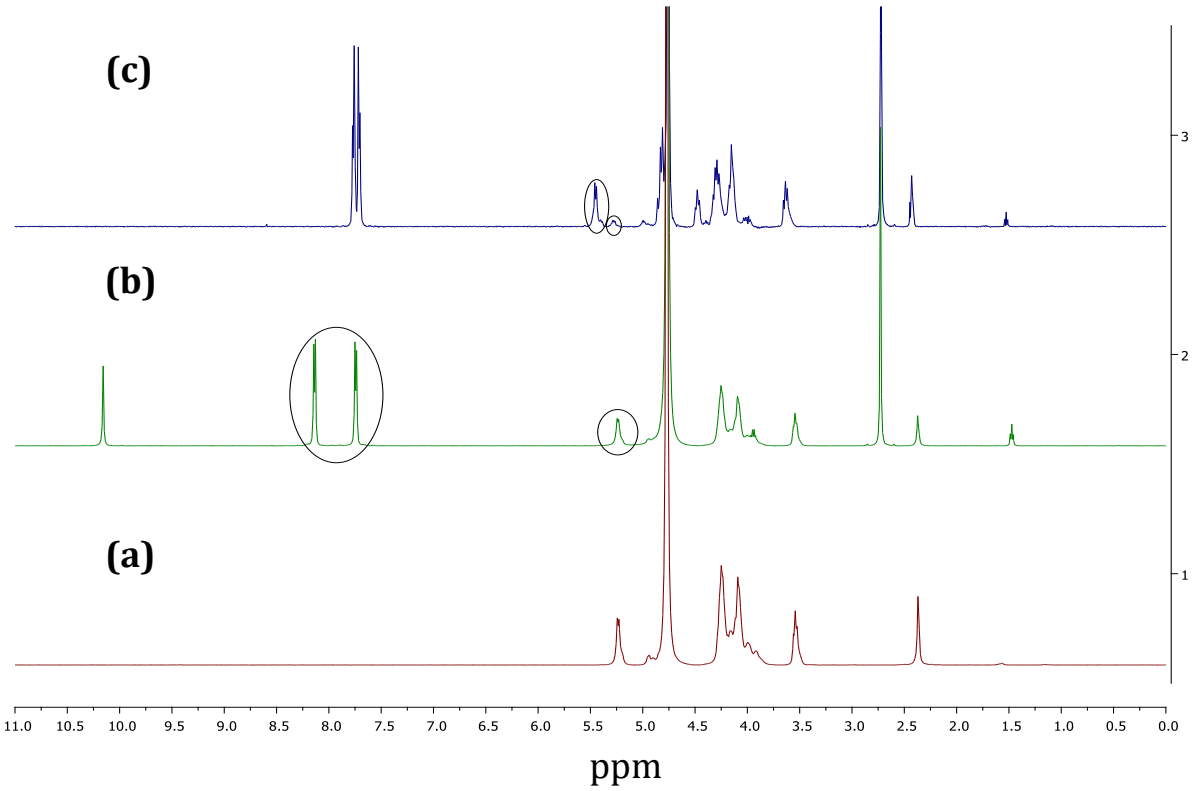

Figure 1. Liquid ^1H NMR spectra of (a) chitosan aerogels **1**; (b) aerogel chitosan derivatives **2a** corresponding to the hydrolysed imine product namely chitosan **1** and para-tolualdehyde **a** (aromatic and anomeric protons are indicated) and (c) **3a** (anomeric protons are indicated).

The chitosan aerogels **1** results from a supercritical CO_2 ($scCO_2$) drying of chitosan gels that is expected to enable the drying without leading to the collapse of the structure. This technic affords a chitosan aerogel with high surface area [41]. N_2 physisorption provides useful information on the volume and size of the mesoporous component of the porosity. The isotherms of the chitosan and the corresponding mesopore size distributions are reported in Fig. 2. The isotherm are of type IV, typical of mesoporous solids (D= [2-50] nm). Surface area A_{BET}

is calculated using points in the [0.05 - 0.3] p/p° range and $\sigma N_2 = 0.162$ nm^2. However, the pore size distributions (PSD) of the aerogels are not limited to mesopores and clearly trespass in the domain of macroporosity (Figure 2).

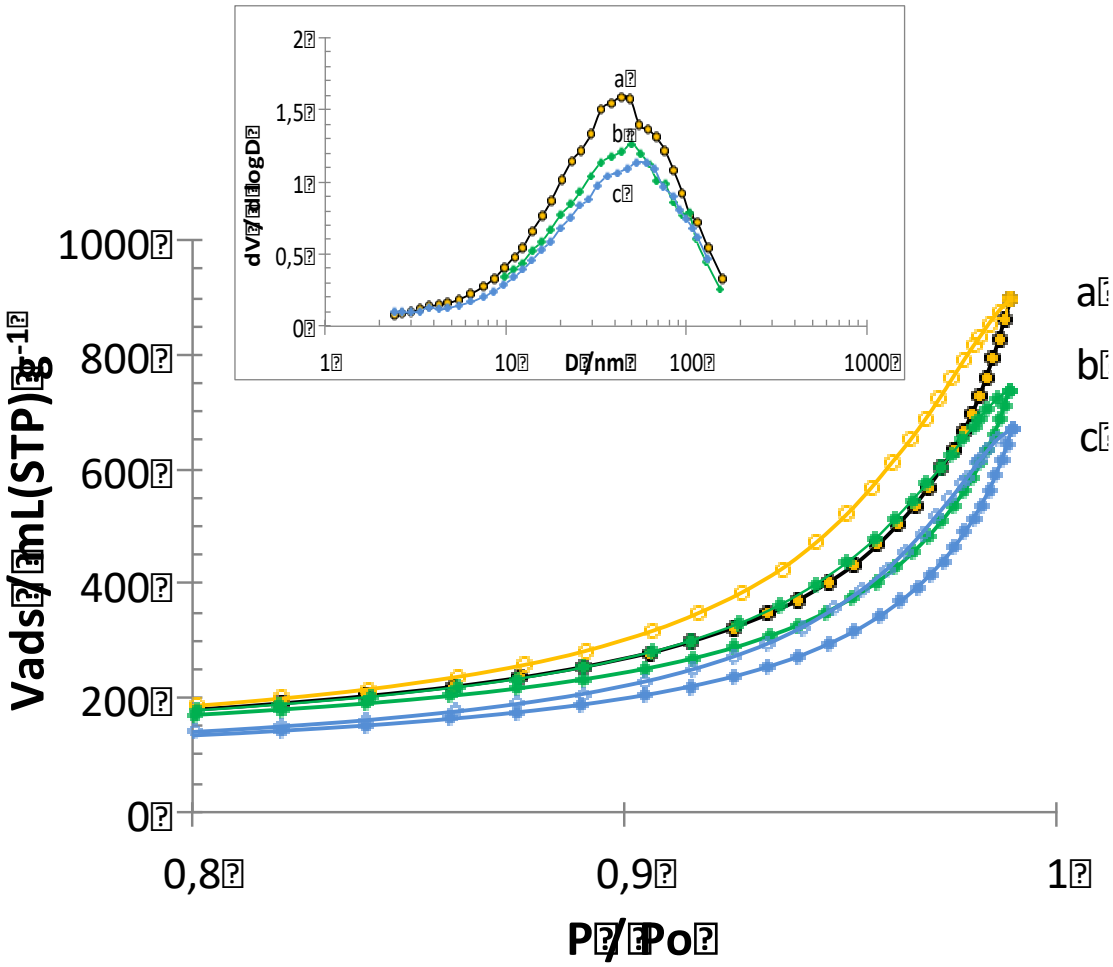

Figure 2: N_2 adsorption isotherms of chitosan aerogel **1** (a) and chitosan derivatives aerogels **2a** (b) and **3a** (c). Full symbol adsorption branch, empty symbol desorption branch.

So the chitosan aerogels behave as material with large surface area of 260 m^2g^{-1}, build in large pores (Table 2).

Table 2: Physical and textural properties of aerogels **1**, **2a** and **3a**

	CrI_{110} (%)	Total pore volume (cm^3g^{-1})	Average mesopore size (nm)	A_{BET} (m^2g^{-1})
1	40,4	1.38	24	262
2a	54,3	1.14	23	270
3a	55,1	1.04	24	203

The textural properties data of the corresponding imines **2a** are reported in Table 2 and showed that this protocol has a low impact on the textural properties of the aerogels, and no shrinkage of the structure was observed. Surface area, total porous volume and PSD (centered nearby 23 nm) are highly preserved (Table 2). The high-magnification image recorded on a chitosane aerogel **1** beads surface evidenced an irregular surface based on fibrous network structure (Figure S1 in the Supporting Information). After modification, the topography of chitosan Schiff base aerogels **2a** is similar.

Figure 3 showed the XRD patterns of chitosan aerogel and chitosan derivatives aerogels.

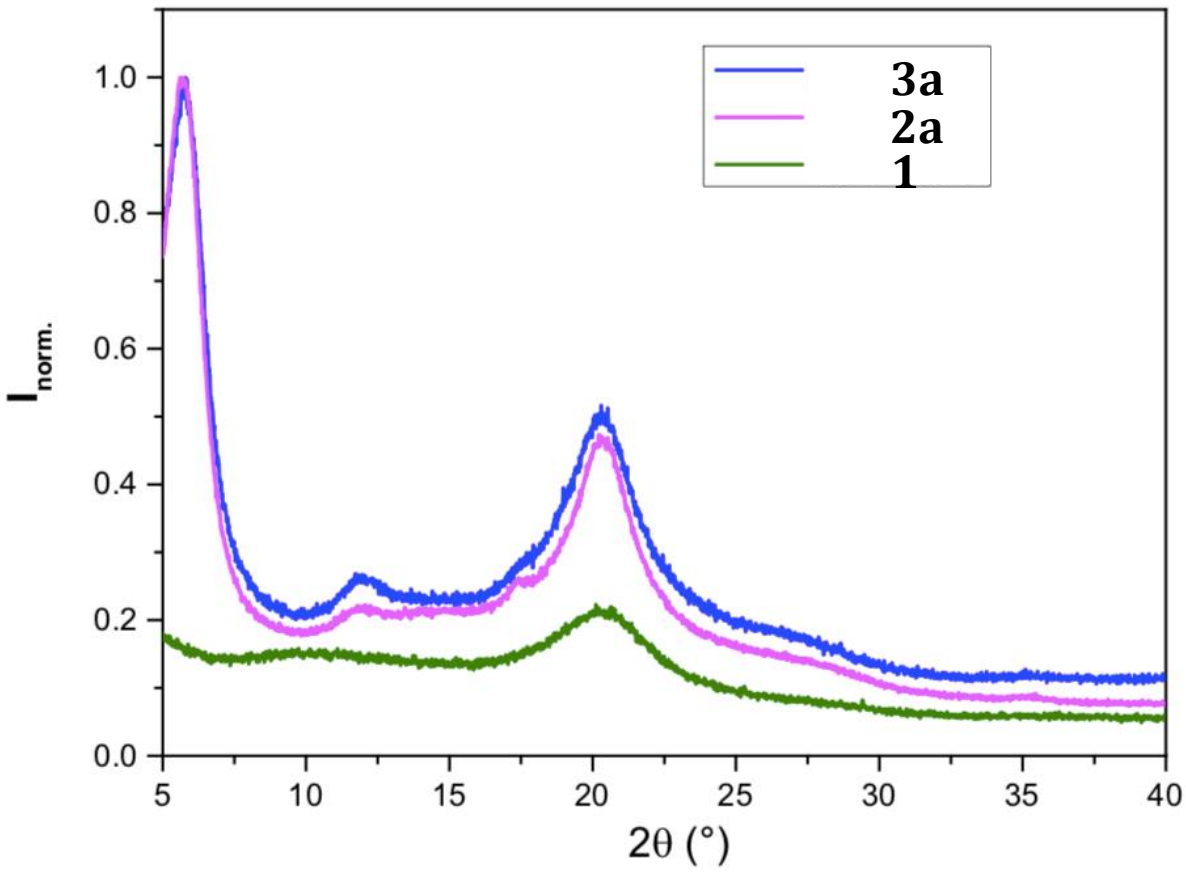

Figure 3. XRD spectra of chitosan aerogels **1** and aerogel chitosan derivatives **2a** and **3a**

XRD of neat chitosan aerogel 1 shows a characteristic peak at about 2θ = 20°, which is attributed to the crystalline structure of chitosan. [42-44]. This peak increased for chitosan derivatives aerogel **2a** and **3a** indicating that the chitosan turned into more crystalline structure. Crystallinity index (CrI) reflecting the regularity of the aggregation state of polymer chains, values were listed in Table 2. The CrI of the chitosan aerogel **1** (40%) was lower than that of **2a**, showing the influence of the aromatic side groups leading to a restructuration of chitosan chains to reach an aggregate architecture with high CrI.

The starting chitosan and chitosan Schiff base aerogels **1** and **2a** were used for the HPLC/SEC studies. The samples were solubilized in the mobile phase, which was 0.2 M AcOH and 0.1 M NH_4OAc to decrease aggregate formation [45]. The determined $\overline{M_n}$ are in the range of 100,000 g mol^{-1} for chitosan derivative aerogel **2a**, being 50,000 g mol^{-1} that of the parent chitosan aerogel **1**. Consequently, no depolymerisation of the parent chitosan under the reaction conditions used takes place.

The textural properties data of the chitosan secondary amine derivative **3a** are reported in Table 2 and showed that the reduction conditions poorly impact the textural properties of chitosan aerogels. As the other derivatives, **3a** aerogels are formed by a loose network with a surface area of 200 m^2g^{-1} and a constant distribution of porous volume at 24 nm (Table 2, Figure 2) corresponding to solids with an important macroporosity. Such open accessible surface is crucial for the catalytic performance of the material affording easy penetration of reactants, diffusivity, transport… . No particular change of the topography of **3a** was evidenced in comparison to those of **2a** (Figure S1 in the Supporting Information).

The XRD spectra of **3a** is similar of **2a** with a cristallinity index of 55% showing the reduction step do not change the chitosan chain packing (Table 2, Figure 3).

Having this very promising protocol in hands, the modification strategy was extended to various aldehyde derivatives (Table 3) bearing aryl ring with electron-donating, withdrawing, boronic ester and phosphine functional groups making use of $NaBH_3CN$ as reductive agent.

Table 3: Synthesis of functionalized Chitosan aerogels **2b-2e** and **3b-3e**

Entry	**Aldehydes**	**Chitosan Schiff base derivatives**[a]	**DS_{imine}**[b]	**Chitosan Amine derivatives**[c]	**DS_{amine}**[b]

1	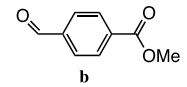 **b**	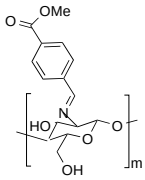 **2b**	99%	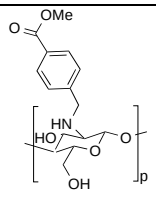 **3b**	67-74%
2	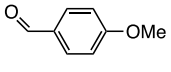 **c**	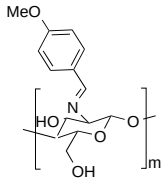 **2c**	99%	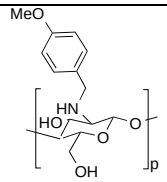 **3c**	83-87%
3	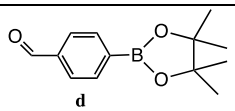 **d**	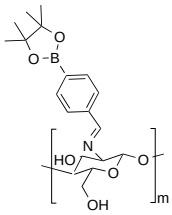 **2d**	99%	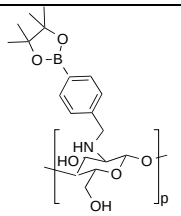 **3d**	86-89%
4	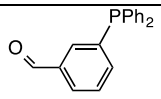 **e**	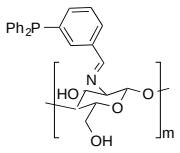 **2e**	98%	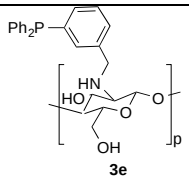 **3e**	nd

[a] General conditions: Chitosan aerogel beads (25mg, 0.127mmol, 1eq), aldehyde (0.508mmol, 4eq) in 1.2mL of absolute EtOH at 60°C under thermal stirring. [b] DS_{imine} and DS_{amine} determined by ^{1}H NMR in DCl/D_2O at 70°C. [c] General conditions: Schiff base **2** (5mg, 1eq), $NaBH_3CN$ (6eq) in 400µL of solvent at room temperature under flipping stirring.

Whatever the electronic nature of aldehyde precursors, the corresponding products were obtained with substitution degree (98-99%) for the imine formation (**2a-b**) and a ratio of reduction ranging from 67 to 87% for the reduced benzylated-products (**3a-b**, entries 1-2). Pleasingly, the boronic ester derivatives **2d-3d** were nicely tolerated with this protocol (entry 3), which offers interesting opportunities on this versatile functional group. This shows the efficiency of these experimental conditions that also afford an easy recovery of the resulting material by simple filtration. As long as the phosphine chitosan aerogels **3e** is concerned, the synthetic sequence started from 3-(diphenylphosphino)benzaldehyde (**e**) and the imine formation succeeded in 99% DS_{imine} to afford **2e**. Importantly, a former procedure was described elsewhere and afford the synthesis of chitosan–2(diphenylphosphino)imine with a low DS [46]. Then the reduction step, performed with $NaBH_3CN$ as reductive agent, afforded a priori the secondary amino chitosan aerogels **3e** as testified by the low remaining amount of starting material **2e**. Unfortunatly, the insolubility of **3e** in the NMR solvents did not allow the determination of the DS_{amine}. However, the IR spectra confirmed the integrity of the phosphine group on the supposing material **3e** by the band at 1434 cm^{-1}. ^{31}P MAS NMR analysis of **3e**

was performed and showed three large peaks at 30 ppm, 11 ppm and -5 ppm [47]. The more intensive peak at -5 ppm is attributed to the phosphine group of **3e**, nevertheless the experimental conditions did afford the partial oxidation of the phosphine indicated by the signal at 30 ppm. Finally, the signal at 11 ppm should be attributed to the phosphine groups of the polymer network involved in hydrogen bonds. These interactions likely explained the lack of solubility of **3e** in various solvents.

3.2 Application to the palladium-catalyzed Tsuji-Trost reaction

Chitosan aerogels structure being well known for their catalytic properties, chitosan aerogels flanked by phosphine moiety with a covalent link were evaluated as a potential heterogenous ligand in palladium catalyzed process [48, 49]. Then, the phosphine chitosan aerogels **2e** in the presence of a palladium species was engaged into a catalytic allylic substitution, one of the most important reaction for carbon–carbon and carbon–heteroatom bond formation [50] (Scheme 2).

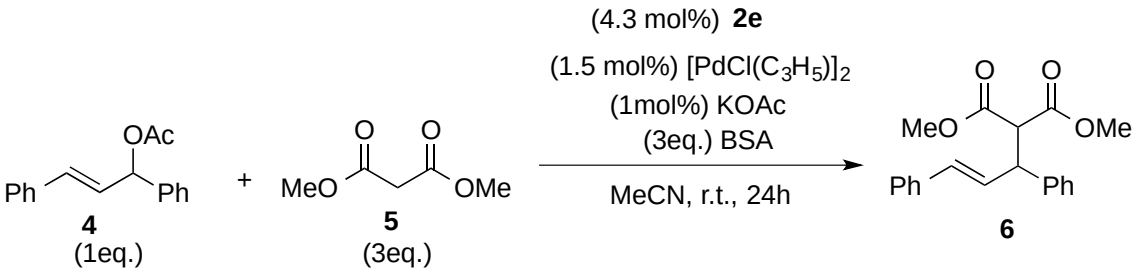

Scheme 2. Palladium catalyzed allylic substitution

Typically, the catalytic aerogels were prepared by mixing in acetonitrile, aerogels **2e** (4.3 mol%) with the palladium source $[PdCl(C_3H_5)]_2$ (1.5 mol%) for 1 hour under Ar. The allylation reaction between (E)-1,3-di- phenyl-3-acetoxyprop-1-ene **4** and dimethyl malonate **5** using BSA as base was selected as a model reaction. The reaction was completed after 24 h at 20°C, affording the expected allylated malonate **6** in good 76% yield (Table 4, entry 1). No enantiomeric excess was mesured by chiral HPLC. The reaction was also performed with chitosan aerogels **1** and **2a**, but in these conditions the corresponding product **6** was not observed, indicating that the no active metallic-complex was formed in this case (Table 4, entries 5 and 6).

Table 4: Pd-catalyzed allylic alkylation of 1,3-diphenylpropenyl acetate **4** with dimethyl malonate **5** using ligands **1**, **2a** and **2e** aerogels[a]

Entry	Ligand	Cycle	Conversion[b]	Yield[d]
1	**2e**	1	100%	76%
2	**2e**	2	100%	80%
3	**2e**	3	100%	73%
4	**2e**	4	73%	nd
5	**1**	1	0%	0%
6	**2a**	1	0%	0%

[a] General conditions: phosphorous Schiff base (8.7mg, 0.0215mmol, 4.3mol%), $[PdCl(C_3H_5)]_2$ (2.7mg, 0.0075mmol, 1.5mol%), KOAc (0.5mg, 0.005mmol, 1mol%), BSA (370µL, 1.5mmol, 3eq), **4** (126mg, 0.5mmol, 1eq) and nucleophile **5** (1.5mmol, 3eq) in 1.2mL of anhydrous and degassed acetonitrile at room temperature under gentle magnetic stirring. [b] Conversion determined by ^{1}H NMR, [d] Isolated yield.

Recycling tests were next performed. They showed a high catalytic activity of the chitosan aerogels for 3 cycles (100% conversion) and a decrease in activity is observed from the fourth run, leading only to a partial conversion of 73% even after 72h (Table 4, entry 4). Detection of palladium by ICP-MS in the crude product **6** showed a low leaching of the metal during the recycling of the catalytic material (< 3%) that did not explain the catalytic deactivation [51]. This analysis showed the high coordination of Pd to the biopolymer-supported Schiff-base ligand and provides evidence of chitosan acting as a good scaffold for Pd^{II} catalyst precursors as already observed in the nice work of Smith and al. who applied successfully chitosan–2(diphenylphosphino)imine ligand in Suzuki-Miyaura and Heck cross-coupling reactions [46].

4. Conclusion

An efficient, mild and non-degradative procedure to prepare secondary amino chitosan derivatives, by reacting chitosan aerogels with arylaldehydes under heterogeneous conditions, is described. This convenient procedure was successfully applied to achieve reaction of several aldehydes with chitosan aerogels to reach high degree of substitution during the imine-formation process. Then, the reduction of chitosan base Schiff derivatives succeeded by using $NaBH_3CN$ as reductive agent and high reduction ratio were obtained (>80%) to afford functional secondary amino chitosans aerogels. The results obtained in this work led to the conclusion that this heterogeneous procedure affords regioselective and quantitative chitosan modifications to get a controlled well-defined macromolecular structure.

Moreover, keeping in mind to preserve the original properties of the chitosan, this study focused on the impact of the experimental conditions on the physical and textural properties of aerogels. Textural analyses showed that the successive heterogeneous chemical modifications of chitosan aerogels do not lead to a collapse of the polymer structure and aerogels keeps a surface of about 250 m^2g^{-1} with a distribution of mesopores centered at 23 nm. XRD analyses showed that, after modification, the chitosan chains were restructured to form more regular aggregate architecture, with a high CrI.

Finally, the heterogeneous and efficient process to prepare macroporous aerogels afforded the synthesis of covalently link phosphine based chitosan aerogels, which were used as phosphorylated ligand in the Pd-catalysed allylic substitution. Such resulted Pd-catalytic opened materials allow by high diffusion properties and afford efficient reaction in mild conditions. The catalyst could be recycled 3 times.

Acknowledgements

The authors acknowledge the financial support of the INC3 M (FR3038), the french Agence Nationale de la Recherche (ANR), through the program "Investissements d'Avenir" (ANR-10-LABX-09-01), LabEx EMC^3, and the region NORMANDIE.

Data Availability

The raw data required to reproduce these findings cannot be shared at this time due to technical and time limitations.

References

[1] G. A. F. Roberts, in Chitin Chemistry, The Macmillan Press Ltd., Hong Kong, 1992.

[2] M.N.V.R. Kumar, A Review of Chitin and Chitosan Applications, React. Funct. Polym. 46 (2000) 1–27.

[3] E. Guibal, Heterogeneous catalysis on chitosan-based materials a review, Prog. Polym. Sci.

30(1) (2005) 71–109.

[4] T. Freier, H.S. Koh, K. Kazazian, M.S. Shoichet, Controlling cell adhesion and degradation of chitosan films by N-acetylation, Biomaterials 26 (2005) 5872–5878.

[5] K. Tomihata and Y. Ikada, In vitro and in vivo degradation of films of chitin and its deacetylated derivatives, Biomaterials, 18 (1997) 567–575.

[6] G. Kravanja, M. Primožicˇ, Ž. Knez and M. Leitge, Chitosan-Based (Nano)Materials for Novel Biomedical Applications, Molecules 24 (2019) 1960-1983.

[7] Q. Mao, C. Xu, N.N. Liu, J.J. Zhu and J. Sheng, Direct electrochemistry of horseradish peroxidase based on biocompatible carboxymethyl chitosan-gold nanoparticle nanocomposite. Biosens. Bioelectron. 22 (2006) 768–773.

[8] C. Hao, L. Ding, X. Zhang and H. Ju, Biocompatible Conductive Architecture of Carbon Nanofiber-Doped Chitosan Prepared with Controllable Electrodeposition for Cytosensing, Anal. Chem. 79 (2007) 4442–4447.

[9] L. Ilium, Chitosan and its use as a pharmaceutical excipient, Pharm. Res. 15 (1998) 1326–1331.

[10] V.R. Sinha, A.K. Singla, S. Wadhawan, R. Kaushik, R. Kumria, K. Bansal and S. Dhawan, Chitosan microspheres as a potential carrier for drugs, Int. J. Pharm. 274 (2004) 1–33.

[11] G. Maurstad, B. T. Stokke, K. M. Vårum, S. P. Strand, PEGylated chitosan complexes DNA while improving polyplex colloidal stability and gene transfection efficiency, Carbohydr. Polym. 94 (2013) 436-443.

[12] S. P. Strand, S. Lelu, N. K. Reitan, C. de Lange Davies, P. Artursson, K. M.Vårum, Molecular design of chitosan gene delivery systems with an optimized balance between polyplex stability and polyplex unpacking, Biomaterials 31 (2010) 975-987.

[13] S. Khattak, F. Wahid, L.P. Liu, S.R. Jia, L. Q. Chu, Y.Y. Xie, Z.X. Li, C. Zhong, Applications of cellulose and chitin/chitosan derivatives and composites as antibacterial materials: current state and perspectives, Appl. Microbiol. Biotechnol. 103 (2019) 1989–2006.

[14] K.N. Hong, Y.P. Na, S.H. Lee, S.P. Meyers, Antibacterial activity of chitosans and chitosan oligomers with different molecular weights. Int. J. Food Microbiol. 74 (2002) 65–72.

[15] E.I. Rabea, E.T. Badawy, C.V. Stevens, G. Smagghe and W. Steurbaut, Chitosan as antimicrobial agent: applications and mode of action, Biomacromolecules 4 (2003) 1457–1465.

[16] N. K. Jaafar, A. Lepit, N. A. Aini, A. Saat, A. M. M. Ali and M. Z. A. Yahya, Effects of lithium salt on chitosan-g-PMMA based polymer electrolytes, Mater. Res. Innov. 15:sup2 (2011) s202-s205.

[17] K. Kurita, Controlled functionalisation of the polysaccharide chitin, Prog. Polym. Sci. 26 (2001) 1921–1971.

[18] E. A. Imam, I. E. T. El-Sayed, M. G. Mahfouz, A. A. Tolba, T. Akashi, A. A. Galhoum and E. Guibal, Synthesis of α-aminophosphonate functionalized chitosan sorbents: effect of methyl vs phenyl group on uranium sorption, Chem. Eng. J. 352 (2018) 1022-1034.

[19] A. Toffey, G. Samaranayake, C.E. Frazier and W.G. Glasser, Chitin derivatives. I. Kinetics of the heat-induced conversion of chitosan to chitin, J. Appl. Polym. Sci. 60 (1996) 75–85.

[20] L.Y. Lim, E. Khor and C.E. Ling, Effects of dry heat and saturated steam on the physical properties of chitosan, J. Biomed. Mater. Res. 48 (1999) 111–116.

[21] H.K. No, S.H. Kim, S.H. Lee, N.Y. Park and W. Prinyawiwatkul, Stability and antibacterial activity of chitosan solutions affected by storage temperature and time, Carbohydr. Polym. 65 (2006) 174-178.

[22] S.E. Howling, Some observations on the effect of bioprocessing on biopolymer stability, J. Drug Target. 18 (2010) 732-740.

[23] Kurita, K. Chitin and Chitosan: Functional Biopolymers from Marine Crustaceans. Mar. Biotechnol. 8 (2006) 203-226.

[24] G. Z. Kyzas and D. N. Bikiaris, Recent modifications of chitosan for adsorption applications: A critical and systematic review, Mar. Drugs 13(1) (2015) 312-337.

[25] A. Pestov and S. Bratskaya, Chitosan and its derivatives as highly efficient polymer ligands, Molecules 21(3) (2016) 330–365.

[26] A. El Kadib and M. Bousmina, Chitosan bio-based organic-inorganic hybrid aerogel microspheres, Chem. Eur. J. 18(27) (2012) 8264-8277.

[27] R. Valentin, B. Bonelli, E. Garrone, F. Di Renzo and F. Quignard, Accessibility of the Functional Groups of Chitosan Aerogel Probed by FT-IR-Monitored Deuteration, Biomacromolecules 8 (2007) 3646-3650.

[28] C. López-Iglesias, J. Barros, I. Ardao, F. J. Monteiro, C. Alvarez-Lorenzo, J. L. Gómez-Amoza and C. A. García-González, Vancomycin-loaded chitosan aerogel particles for chronic wound applications, Carbohydr. Polym. 204 (2019) 223-231.

[29] Z. Li, L. Shao, Z. Ruan, W. Hu, L. Lu and Y. Chen, Converting untreated waste office paper and chitosan into aerogel adsorbent for the removal of heavy metal ions, Carbohydr. Polym. 193 (2018) 221-227.

[30] A. Li, R. Lin, C. Lin, B. He, T. Zheng, L. Lu and Y. Cao, An environment-friendly and multi-functional absorbent from chitosan for organic pollutants and heavy metal ion, Carbohydr. Polym. 148 (2016) 272-280.

[31] A. El Kadib Chitosan as a sustainable organocatalyst: A concise overview, ChemSusChem 8(2) (2015) 217–244.

[32] O. Mahé, J.F. Brière and I. Dez, Chitosan: an Upgraded Polysaccharide Waste for Organocatalysis, Eur. J. Org. Chem. 12 (2015) 2559-2578.

[33] S. Keshipour and S. S. Mirmasoudi, Cross-linked chitosan aerogel modified with Au: Synthesis, characterization and catalytic application, Carbohydr. Polym. 196 (2018) 494-500.

[34] F. Li, L. G. Ding, B. J. Yao, N. Huang, J. T. Li, Q. J. Fu and Y. B. Dong, Pd loaded and covalent-organic framework involved chitosan aerogels and their application for continuous flow-through aqueous CB decontamination, J. Mater. Chem. A 6(24) (2018) 11140-11146.

[35] M. Chtchigrovsky, A. Primo, P. Gonzalez, K. Molvinger, M. Robitzer, F. Quignard and F. Taran, Functionalized Chitosan as a Green, Recyclable, Biopolymer-Supported Catalyst for the [3+2] Huisgen Cycloaddition, Angew. Chem. Int. Ed., 48, (2009) 5916 -5920.

[36] S. Jatunov, A. Franconetti, R. Prado-Gotor, A. Heras, M. Mengíbar, F. Cabrera-Escribano,

Fluorescent imino and secondary amino chitosans as potential sensing biomaterials, Carbohydr. Polym. 123 (2015) 288–296.

[37] D. B. Williams, M. Lawton, Drying of Organic Solvents: Quantitative Evaluation of the Efficiency of Several Desiccants, J. Org. Chem. 75 (2010) 8351-8354.

[38] B. Focher, A. Naggi, G. Torri, A. Cosanni and M. Terbojevich, Chitosans from Euphausia Superba 2: Characterization of solid state structure, Carbohydr. Polym. 18 (1992) 43-49.

[39] L. Picton, G. Mocanu, D. Mihai, A. Carpov and G. Muller, Chemically modified exopolysaccharide pullulans: physico-chemical characteristics of ionic derivatives, Carbohydr. Polym. 28 (1995) 131-6.

[40] J. Baudoux, K. Perrigaud, P.J. Madec, A.C. Gaumont and I. Dez, Development of new SILP catalysts using chitosan as support, Green Chem. 9 (2007) 1346-1351.

[41] M. Robitzer, F. Di Renzo and F. Quignard, Natural materials with high surface area. Physisorption methods for the characterization of the texture and surface of polysaccharide aerogels, Micropor. Mesopor. Mat. 140 (2011) 9–16.

[42] K. V. Harish Prashanth, F. S. Kittur and R. N. Tharanathan, Solid state structure of chitosan prepared under different N-deacetylating conditions, Carbohydr. Polym. 50 (2002) 27-33.

[43] N. Zhang, H. Qiu, Y. Si, W. Wang and J. Gao, Fabrication of highly porous biodegradable monoliths strengthened by graphene oxide and their adsorption of metal ions, Carbon 49 (2011) 827–837.

[44] X. Yang, Y. Tu, L. Li, S. Shang and X. M. Tao, Well-Dispersed Chitosan/Graphene Oxide Nanocomposites, ACS Appl. Mater. Interfaces 2 (2010) 1707–1713.

[45] G. Lamarque, J.M. Lucas, C. Viton and A. Domard, Physicochemical behavior of homogeneous series of acetylated chitosans in aqueous solution: role of various structural parameters, Biomacromolecules 6(1) (2005) 131-42.

[46] B.C.E. Makhubela, A. Jardine and G. S. Smith, Pd nanosized particles supported on chitosan and 6-deoxy-6-amino chitosan as recyclable catalysts for Suzuki–Miyaura and Heck cross-coupling reactions, Applied Catalysis A: General 393 (2011) 231–241.

[47] J. Bliimel, Reactions of phosphines with silica : A solid-state NMR study, Inorg. Chem., 33 (1994) 5050-5056.

[48] R. Moucel, K. Perrigaud, J.M. Goupil, P.J. Madec, S. Marinel, E. Guibal, A.C. Gaumont, I. Dez, Importance of the Conditioning of the Chitosan Support in a Catalyst-Containing Ionic Liquid Phase Immobilised on Chitosan: The Palladium-Catalysed Allylation Reaction Case, Adv. Synth. Catal. 352 (2010) 433-439.

[49] A. Ricci, L. Bernardi, C. Gioia, S. Vierucci, M. Robitzer and F. Quignard, Chitosan aerogel: a recyclable, heterogeneous organocatalyst for the asymmetric direct aldol reaction in water, Chem. Commun. 46 (2010) 6288–6290.

[50] J. Tsuji, in Palladium Reagents and Catalysts, Wiley and Sons, New York, 1995.

[51] F. Vittoz, H. El Siblani, A. Bruma, B. Rigaud, X. Sauvage, C. Fernandez, A. Vicente, N. Barrier, S. Malo, J. Levillain, A.C. Gaumont and I. Dez, Insight in the Alginate Pd-Ionogels_Application to the Tsuji–Trost Reaction, ACS Sustain. Chem. Eng., 6 (4) (2018) 5192-5197.